An Earthen Sill as a Measure to Mitigate Salt Intrusion in Estuaries

Hendrickx, Gijs G.; Manuel, Laura A.; Pearson, Stuart G.; Aarninkhof, Stefan G.J.; Meselhe, Ehab A.

DOI
10.1007/s12237-024-01359-2

Publication date
2024

Document Version
Final published version

Published in
Estuaries and Coasts

Citation (APA)
Hendrickx, G. G., Manuel, L. A., Pearson, S. G., Aarninkhof, S. G. J., & Meselhe, E. A. (2024). An Earthen Sill as a Measure to Mitigate Salt Intrusion in Estuaries. *Estuaries and Coasts*, *47*(5), 1199-1208. https://doi.org/10.1007/s12237-024-01359-2

Estuaries and Coasts
https://doi.org/10.1007/s12237-024-01359-2

An Earthen Sill as a Measure to Mitigate Salt Intrusion in Estuaries

Gijs G. Hendrickx[1] · Laura A. Manuel[2] · Stuart G. Pearson[1] · Stefan G. J. Aarninkhof[1] · Ehab A. Meselhe[2]

Received: 15 November 2023 / Revised: 4 April 2024 / Accepted: 7 April 2024

Abstract
At a global scale, deltas are vital economic hubs, in part due to the combination of their access to inland regions via river systems with their proximity to sea. However, with the sea in close vicinity also comes the threat of freshwater contamination by saline seawater, especially during droughts. This study explores the potential of a mitigation measure to estuarine salt intrusion, namely the construction of a (temporary) earthen sill—a measure implemented in the Lower Mississippi River near New Orleans (LA, USA). This study suggests design guidelines on how a sill can be used to mitigate estuarine salt intrusion: the design should focus on the longitudinal placement and the height of the sill, and the mitigating efficiency of the sill reduces with increasing tidal range. Overall, a (temporary) sill has great potential to reduce salt intrusion in salt wedge estuaries if there is sufficient water depth available.

Keywords Estuaries · Nature-based solutions · Salt intrusion · Salt wedge · 3D modelling

Introduction

Worldwide, deltas are among the most densely populated and heavily utilised regions with 40% of the population living within 100 km from the coastline (Maul and Duedall 2019). Due to their closeness to the sea, these regions largely rely on freshwater supply from rivers for their drinking water, which are susceptible to salt contamination (Costall et al. 2018).

Especially during a drought, this much-needed freshwater supply is lacking, causing a direct and indirect reduction of the freshwater availability: directly by a reduced inflow of freshwater to the system and indirectly by an enhanced salt intrusion (e.g. Gong and Shen 2011; Lerczak et al. 2009) causing the contamination of the available freshwater. A recent example includes the severe and persistent drought event in the Lower Mississippi River (LMR), causing an unprecedented advancement of the salt wedge, which threatened to contaminate drinking water intakes of the City of New Orleans (LA, USA). Such strains on freshwater—i.e. water stress—are expected to increase in frequency due to the changing climate (Distefano and Kelly 2017; Veldkamp et al. 2015). Therefore, it is important to develop salt intrusion mitigation measures.

One such mitigation measure to safeguard the freshwater availability is the construction of a temporary earthen sill—i.e. a submerged, broad-crested dam from local sediments—during a (severe) drought event. The US Army Corps of Engineers has been experimenting with this concept in the LMR near New Orleans giving good results under exceptional drought conditions (Fagerburg and Alexander 1994; Johnson et al. 1987) and was forced to construct the sill again recently, namely October 2022 and August 2023. Here, a sill is constructed with locally retrieved sediments that remain in place during low flow conditions in order to block the saline water from propagating landward until the sill in naturally flushed away during moderate and high flow conditions, restoring the bed to its pre-intervention state (Fagerburg and Alexander 1994). This sill aims to halt the upstream

Communicated by Jessica R. Lacy

Highlights
1. A (temporary) earthen sill is an effective measure to mitigate salt intrusion in salt wedge estuaries.
2. The location and height of the sill largely determine the effectiveness of a sill as mitigation measure.
3. The sill is most effective in mitigating salt intrusion when salt transport is dominated by estuarine circulation.

✉ Gijs G. Hendrickx
G.G.Hendrickx@tudelft.nl

[1] Department of Hydraulic Engineering, Delft University of Technology, Delft, The Netherlands

[2] Department of River-Coastal Science and Engineering, Tulane University, New Orleans, LA, USA

Published online: 28 May 2024

propagation of the salt wedge driven by estuarine circulation and thereby attempts to exploit natural processes to achieve its goal. As the estuarine circulation promotes stratification in the estuary, i.e. saline water flowing underneath freshwater, a sill aims to halt the upstream-flowing saline water by blocking the lower part of the water column while allowing for continuation of navigation operations and enabling the discharge of freshwater downstream higher in the water column. Therefore, the construction of the temporary sill in the LMR during a drought can be considered a nature-based solution, where its temporary characteristic is an important component: A permanent sill|equivalent to a submerged weir|would obstruct the flow during non-drought conditions, increasing flood risk in its vicinity (e.g. Villemonte 1947).

Despite the successes of a temporary earthen sill in the LMR, there is—perhaps surprisingly—not much uptake in other estuaries globally. A more general uptake of this strategy is hampered by a lack of knowledge on the processes causing the mitigation of salt intrusion due to sill construction. Thus, the export of this concept to other estuarine systems requires understanding on how such a sill performs under a variety of fluvial and coastal conditions.

The aim of this paper is to determine under which boundary and geomorphological conditions a sill is a viable (nature-based) solution to mitigate salt intrusion. In this way, we address the research question of how a sill mitigates salt intrusion in an estuary. The findings from this research subsequently result in design guidelines on the implementation of a sill as mitigation measure for salt intrusion.

Method

The viability of a sill as a (nature-based) solution to mitigate salt intrusion is assessed by means of numerical experiments. Idealised estuarine morphologies are used to explore various options using a parametric design (Idealised Estuarine Geomorphology) to (1) carefully control the model parametrisation, (2) isolate the various governing processes, and (3) reduce the computational costs. In analysing the estuarine responses to the sill and in determining the processes driving these different responses, a salt flux decomposition is performed (Salt Flux Decomposition).

Numerical Experiments

The idealised estuaries represent both a generally representative morphology and a morphology representative for the LMR, bridging the step from the idealised estuaries to the LMR. Both estuarine layouts were based on a convergent estuary, where the measures of the 'General' estuaries were chosen such that with the same geomorphology we could represent various estuarine classes (Table 2). The hydrodynamic modelling software used for these numerical experiments is briefly introduced in "Hydrodynamic Model" section.

Idealised Estuarine Geomorphology

For the idealised estuarine geomorphology, a parametric design of an estuary with a sill is used (Fig. 1). The boundary conditions are prescribed by a constant river discharge and a single tidal component, i.e. the tidal signal is represented by a monochromatic sine wave with an amplitude and period as described in Table 1: a semi-diurnal tide for the 'General' estuary and a diurnal tide for the LMR-representation. Therefore, we assessed quasi-steady states of an estuary.

The water depth on top of the sill is described relative to the channel depth (Table 1). As this study only considers sills and no gullies, this ratio does not exceed one: $\delta_s \leq 1$. The sill height is subsequently defined as:

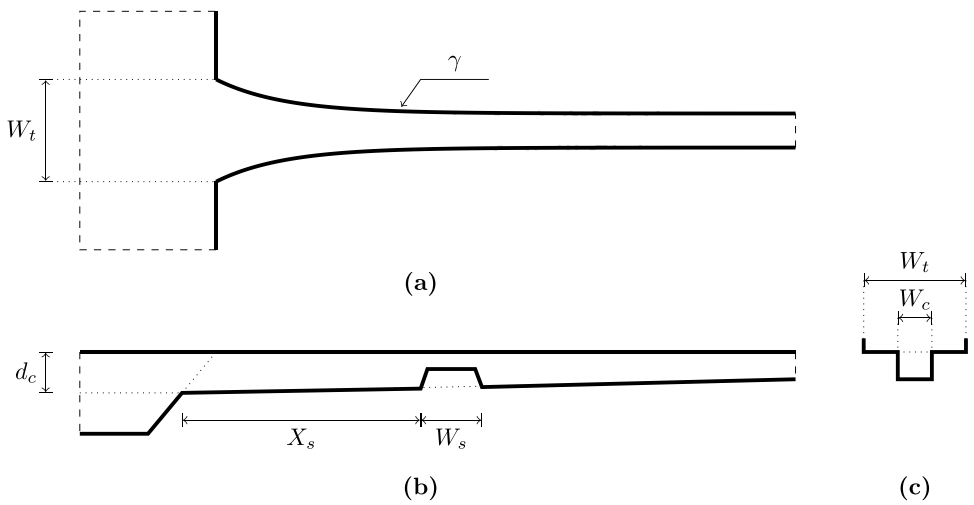

Fig. 1 Parametric model design. **a** Plan view; **b** longitudinal cross-section; and **c** lateral cross-section. The meanings of the symbols are presented in Table 1, except for W_t and X_s: W_t is the total width, $W_t = W_c + W_f$; and X_s the sill location, $X_s = (1 + \lambda_s)L_s^0$

Table 1 Input parameters for the idealised simulations including their values/ranges and corresponding units. The values in the column *General* are used for the model simulations as labelled in Table 2

	Parameter	Symbol	Values		Unit
			General	LMR	
Forcing	Tidal range	a	0.5 – 4.0	0.6	m
	Tidal period	T_t	12	24	h
	River discharge	Q	200 – 1,000	4,950	$m^3\ s^{-1}$
Geomorphology	Estuary length	L_e	200,000	200,000	m
	Channel depth	d_c	13.0	30.5	m
	Channel width	W_c	500	750	m
	Flat depth	d_f	–	15.0	m
	Flat width	W_f	0	500	m
	Bottom friction	n	0.023	0.010	$s\ m^{-1/3}$
	Convergence	γ	40	40	$\times 10^{-6}\ m^{-1}$
Sill	Sill depth ratio[a]	δ_s	0.1 – 1.0	0.5	–
	Sill length	W_s	1,000	200	m
	Sill location ratio[b]	λ_s	−0.25 – 0.25	−0.25 – 0.25	–

[a] The sill depth is defined as ratio to the channel depth: $d_s = \delta_s d_c$

[b] The sill location is defined with respect to the salt intrusion length without a sill (L_s^0): $X_s = \left(1 + \lambda_s\right)L_s^0$

$$h_s = \left(1 - \delta_s\right)d_c.$$

where δ_s is the sill depth ratio [–]; and d_c the channel depth [m].

We consider the location of the sill relative to the salt intrusion length without a sill (L_s^0) by varying the location ratio (λ_s, Table 1):

$$X_s = \left(1 + \lambda_s\right)L_s^0$$

where λ_s is the sill location ratio [–]; and L_s^0 the reference salt intrusion length [m].

The numerical experiments consisted of three sets of analyses: (1) responses for three estuary classes, (2) responses for tidal influence in salt wedge systems, and (3) responses for a representation of the LMR. Table 1 shows an overview of all input parameters for these numerical experiments, where the boundary conditions for the first two sets of experiments are presented in Table 2, including their estuary classes.

This study implemented a rectangular cross-section despite any potential influences this may have on the subtidal flow (e.g. Schulz et al. 2015; Valle-Levinson 2008). A rectangular cross-section allowed us to focus on the longitudinal effects of the laterally oriented obstruction, namely the sill. Furthermore, previous research has shown that lateral variations in the cross-sectional profile have a limited impact on the salt intrusion length, which is dominated by other, more relevant estuary-scale variables; thus, their effects on the salt intrusion length are on a lesser order of magnitude (Hendrickx et al. 2023).

Hydrodynamic Model

The implemented hydrodynamic modelling software for all numerical experiments is Delft3D Flexible Mesh (Kernkamp et al. 2011). This modelling software implements the hydrostatic pressure assumption and solves for the Reynolds-averaged Navier–Stokes equations. Turbulent structures are resolved using the k-ϵ turbulence closure model.

Due to the focus on salt intrusion, three-dimensional models were used with a combination of Z- and σ-layers to discretise the vertical axis; Z-layers are known to be best suited for numerically solving salt wedge dynamics (e.g. Stelling and van Kester 1994), while σ-layers are preferred for representing water levels as they follow the water surface (Deltares 2022). In addition, σ-layers may cause numerical mixing at steep slopes—such as a sill—due to hydrostatic inconsistency (Haney 1991). Thus, the vertical discretisation implemented in this study contains Z-layers (static vertical discretisation) for the majority of the water column topped with σ-layers (dynamic vertical discretisation) to accommodate water level changes.

Table 2 Boundary conditions per estuary configuration with the estuary class based on the estuarine Richardson number (Ri_E) and Geyer and MacCready (2014, GM14)

Label	a [m]	Q [$m^3 s^{-1}$]	Ri_E	GM14
Salt wedge/micro-tidal	0.5	1000	Salt wedge	Salt wedge
Partially mixed	3.0	500	Partially mixed	Partially mixed
Well-mixed	4.0	200	Well-mixed	Partially mixed
Macro-tidal	4.0	1000	Partially mixed	Time-dependent salt wedge

For the description of the model domain, the distinction is made between the shelf and estuarine subdomains. The shelf is a square of 30 × 30 km with a grid resolution of 62.5 × 62.5 m near the estuarine mouth, which decreases to the domain's boundaries reaching a resolution of 1000 × 1000 m. The estuarine domain is 200 km long, and its width converges from the mouth (Table 1) to an upstream minimum based on the river discharge (similar to Hendrickx et al. 2023); upstream widths vary between approximately 200 and 980 m. The grid resolution at the mouth corresponds with the shelf subdomain—i.e. 62.5 × 62.5 m—and coarsens towards the upstream boundary, where it is < 250 × 1000 m; the < 250 m follows from the grid being squeezed by the lateral deformation induced by the convergence. The extent of the high resolution in the estuarine subdomain is set to surpass both the sill's placement (X_s) and salt intrusion length (L_s) to ensure that the area of interest is within the high resolution grid. Nesting between different grid resolutions was accommodated for by triangular grid cells. This parametric design of the estuary and the model's grid are similar to Hendrickx et al. (2023).

The model simulation duration varied per estuary class due to differing spin-up times, which varied from 8 days (salt wedge) to 59 days (well-mixed). Subsequently, the quasi-steady state analyses were based on the last day of the simulation, i.e. the ninth day (salt wedge) or the 60th day (well-mixed), which included either two tidal cycles (semi-diurnal) or a single tidal cycle (diurnal).

The numerical experiments did not consider any morphological dynamics, i.e. the bed level was stationary. Thus, the flushing of the sill—as mentioned in "Introduction" section—was not included.

Salt Flux Decomposition

To explain the differences in system responses to the introduction of a sill, we performed a salt flux decomposition. Such a decomposition discriminates the various driving mechanisms of the sub-tidal salt flux (e.g. Dronkers and van de Kreeke 1986; Lerczak et al. 2006; Ralston et al. 2010). The total salt flux can be written as

$$F = \overline{\int usdA} \tag{1}$$

where u is the flow velocity [ms^{-1}], s the salinity [psu], and A the cross-sectional area [m^2]. The over-line indicates tidal averaging, i.e. taking the temporal average over a tidal cycle.

This salt flux can be decomposed in four components (Garcia et al. 2021): the salt flux related to (1) net flow, (2) tidal oscillation, (3) estuarine circulation, and (4) time-dependent shear. The relevant velocity and salinity components are defined by Eqs. 2a to 2e, where $\mathcal{X}$ represents either the flow velocity, u, or the salinity, s:

$$\mathcal{X}_1 = \frac{\overline{\int \mathcal{X}\,\mathrm{d}A}}{\overline{\int \mathrm{d}A}} \tag{2a}$$

$$\mathcal{X}_2 = \frac{\int \mathcal{X}\,\mathrm{d}A}{\int \mathrm{d}A} - \mathcal{X}_1 \tag{2b}$$

$$\mathcal{X}' = \mathcal{X} - \mathcal{X}_2 - \mathcal{X}_1 \tag{2c}$$

$$\mathcal{X}_3 = \frac{\overline{\mathcal{X}'\,\mathrm{d}A}}{\overline{\mathrm{d}A}} \tag{2d}$$

$$\mathcal{X}_4 = \mathcal{X}' - \mathcal{X}_3 \tag{2e}$$

such that $u = u_1 + u_2 + u_3 + u_4$. Subsequently, the total salt flux (i.e. Eq. 1) can be represented by the sum of these four components:

$$F \approx \underbrace{u_1 s_1 \overline{\int dA}}_{F_1} + \underbrace{\overline{u_2 s_2 \int dA}}_{F_2} + \underbrace{\int u_3 s_3 d\overline{A}}_{F_3} + \underbrace{\overline{\int u_4 s_4 dA}}_{F_4} \tag{3}$$

where F_i corresponds with the salt flux component as previously numbered: F_1 relates to the net flow; F_2 to the tidal oscillation; F_3 to the estuarine circulation; and F_4 to the time-dependent shear.

In general, the landward salt fluxes are dominated by the components related to the tidal oscillation (F_2) and the estuarine circulation (F_3), as (1) the net flow (F_1) always results in a seaward directed salt flux, and (2) the time-dependent shear (F_4) is considered a residual term—which is generally an order of magnitude smaller than the other components—and therefore often excluded from the analysis or included in either F_2 or F_3 (e.g. Dronkers and van de Kreeke 1986; Garcia and Geyer 2023; Lerczak et al. 2006; Ralston et al. 2010).

Results

The results presented in this section are grouped by the three sets of analyses, as introduced in "Idealised Estuarine Geomorphology" section: (1) estuary classes (Estuary Classes), (2) tidal influence in salt wedge systems (Tidal Influence on Salt Wedge), and (3) LMR-representation (Lower Mississippi River).

In all results, the salt intrusion length (L_s) is defined as the tidal- and depth-averaged 1-psu isohaline. Despite our

focus on salt wedge estuaries, this value is considered representative; the depth-averaged salt intrusion is highly correlated with both the depth-minimum and depth-maximum salt intrusion length. To compare the various estuarine responses to the introduction of a sill, we have normalised all salt intrusion lengths with the reference case, i.e. the salt intrusion length in the same estuary without a sill (L_s^0).

By default, the height of the sill is half the water depth, i.e. $\delta_s = 0.5$. This has been found to be the generally most effective sill height in limiting the salt intrusion (Fig. 4) and thus highlights the differences between estuarine responses.

Estuary Classes

The influence of the placement of a sill changes considerably from a salt wedge system (large effect) to a well-mixed estuary (small effect; Fig. 2). In general, the salt intrusion length reduces with seaward placement of the sill. However, the overall influence of the sill on the salt intrusion in the well-mixed estuary is limited. The estuarine response for this estuary class shows fluctuations in its response (Fig. 2). These fluctuations are the result of the large tidal oscillation of the salt intrusion length: The variation in salt intrusion length over the tidal cycle (noise, ±30%) exceeds the variation in salt intrusion length as function of the sill placement (signal, ±5%). This means that the signal is highly distorted, and the noise dominates the output. Due to this insensitivity of the salt intrusion to the sill location, sills are not a relevant mitigation measure in well-mixed estuaries.

In addition, Fig. 2 shows that the sill can both reduce and enhance the salt intrusion length. This means that when placed incorrectly, a sill might act counterproductively in mitigating salt intrusion. Especially for the partially mixed estuary, a sill has to be placed relatively far seaward to reduce salt intrusion; in case of the salt wedge estuary, the salt intrusion length is almost completely defined by the placement of the sill.

Given that the salt intrusion length is most strongly modified by a sill in salt wedge systems (Fig. 2) and motivated by real-life implementation is such a system, we focus in the remainder of this study on these salt wedge estuaries.

Tidal Influence on Salt Wedge

These results consider the influence of the tidal range on salt wedge estuaries, i.e. the micro- and macro-tidal systems as labelled in Table 2. Both variations in the longitudinal sill placement (X_s) and the sill height (h_s) are considered; the sill length (W_s) has been found of less relevance on the salt intrusion, as later discussed in "Sill Dimensions" section.

Figure 3 shows that the salt intrusion is reduced if the sill is placed seaward of the reference salt intrusion ($X_s < L_s^0$), but enhanced if the sill is placed landward ($X_s > L_s^0$). This holds for both tidal range values and indicates a difference between the partially mixed estuary shown in Fig. 2 and the macro-tidal estuary presented in Fig. 5.

Aside from this general response between the sill location and the salt intrusion length, the tidal range clearly

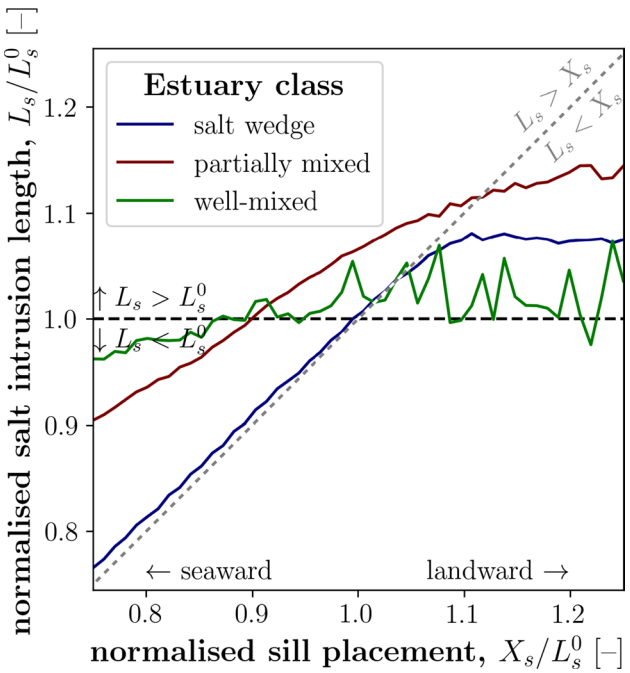

Fig. 2 Salt intrusion length for three estuary classes (Table 2) as function of the sill placement ($\delta_s = 0.5$)

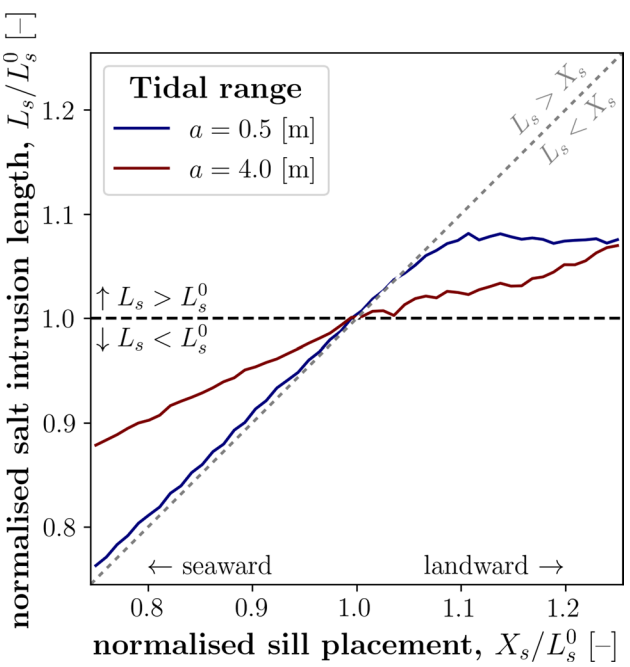

Fig. 3 Salt intrusion length for various sill placements as well as a small and large tidal range ($\delta_s = 0.5$)

has an influence on how the salt intrusion is reduced by the sill. While the sill halts the salt intrusion for a small tidal range ($a = 0.5$ m), it is overspilled for a large tidal range ($a = 4.0$ m). Despite the sill overspilling, it reduces the salt intrusion length compared to the reference case—i.e. without sill.

The effectiveness of reducing the salt intrusion by a sill is also influenced by the height of the sill. How the salt intrusion is affected by the sill height is, again, related to the tidal range (Fig. 4). For both a small and a large tidal range, the salt intrusion reduces with sill height for $h_s/d_c \leq 0.5$. Once the sill height exceeds half the water depth ($h_s/d_c > 0.5$), the response deviates: For a small tidal range ($a = 0.5$ m), the salt intrusion length remains approximately equal to the sill location, and for a large tidal range ($a = 4.0$ m), the salt intrusion length increases beyond the reference case, i.e. without a sill.

The different responses due to the changes in tidal range can be explained by decomposing the sub-tidal salt fluxes. These salt flux components have been determined for the idealised model simulations without a sill for both tidal range values. The addition of a sill causes some minor irregularities in the salt fluxes around the sill's location (not shown) but does not affect the overall spatial distribution of the salt flux components. These spatial distributions are displayed in Fig. 5 in which the most relevant salt flux components are highlighted: tidal oscillation and estuarine circulation (F_2 and F_3 in Eq. 3, resp.). The longitudinal distance is normalised by the salt intrusion length, as beyond this point all salt fluxes are zero, and the salt fluxes are normalised with their maximum absolute value to better compare between different estuaries—i.e. the salt fluxes are normalised such that $F_i \in [-1, 1]$.

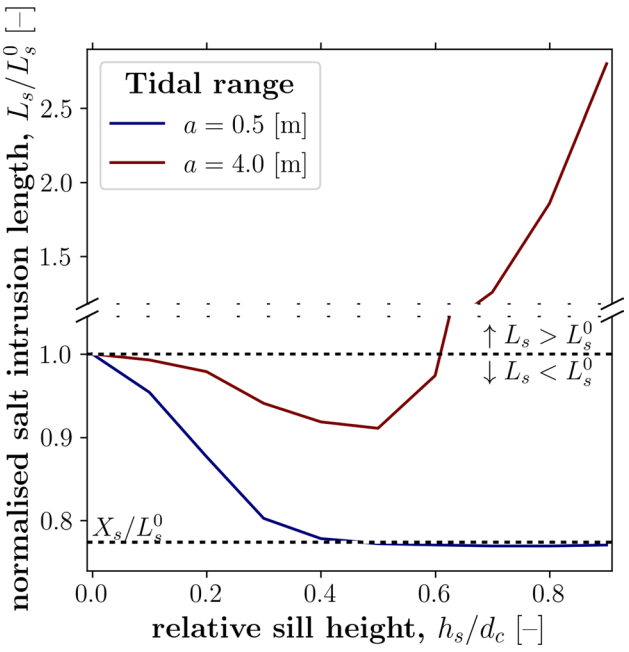

Fig. 4 Salt intrusion length for various sill heights for both tidal ranges. Note the break in the y-axis

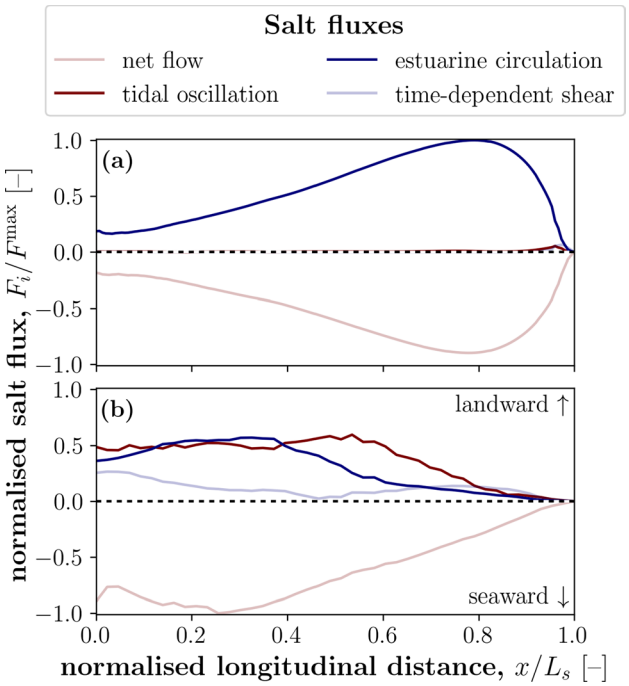

Fig. 5 Spatial distribution of salt flux components for **a** a small tidal range, $a = 0.5$ m; and **b** a large tidal range, $a = 4.0$ m. These figures show the salt fluxes for the reference cases, i.e. without a sill

Figure 5 shows a clear difference between the dominant salt flux components based on the tidal range while both representing salt wedge systems. The landward salt flux is fully driven by the estuarine circulation for a small tidal range with negligible contributions of the other components (Fig. 5a). For a large tidal range, the landward salt flux is largely shared between the estuarine circulation and tidal oscillation, and a minor contribution of the time-dependent shear component (Fig. 5b).

Lower Mississippi River

As a sill has been successfully implemented in the LMR in the past, an idealised representation of the LMR is included (Table 1). The LMR is forced by a very small diurnal tide and is river-dominated, resulting in a strong salt wedge. Figure 6 presents the response of the idealised LMR with the results as presented in Fig. 3 as reference. The idealised LMR shows a similar behaviour of the salt intrusion length with respect to the sill placement: The salt intrusion is reduced when the sill is placed seaward of the reference salt intrusion length ($X_s < L_s^0$), and vice

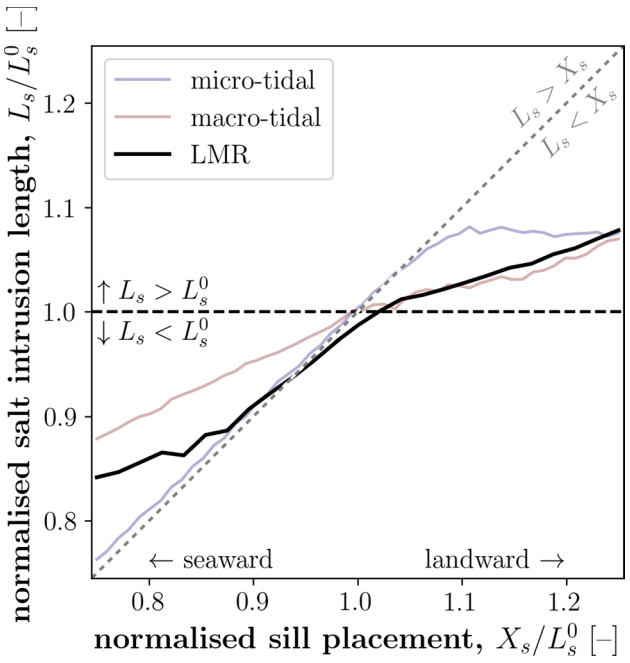

Fig. 6 Salt intrusion length for various sill placements for the idealised representation of the LMR

versa. This behaviour is in line with our other results (Fig. 3) despite the differences in estuarine geomorphology (Table 1), such as the introduction of shallow areas.

For $X_s < L_s^0$, the idealised LMR behaves similarly to the micro-tidal system (blue line in Fig. 6), which is expected from the similar spatial pattern of salt flux components (Fig. 7). However, the enhancement of the salt intrusion length for $X_s > L_s^0$ is not as profound as the micro-tidal system.

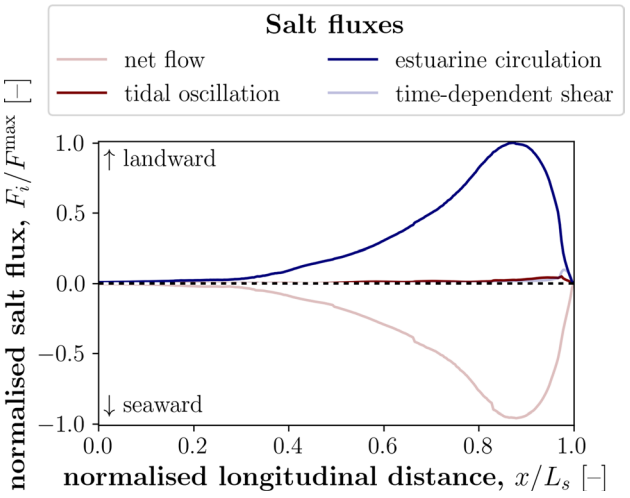

Fig. 7 Spatial distribution of salt flux components for the idealised LMR. This figure shows the salt fluxes for the reference case, i.e. without sill

Discussion

We concluded from Fig. 2 that sills are most viable in (time-dependent) salt wedge systems. Therefore, in "Sill Placement" and "Sill Dimensions" sections, we focus on these estuary types, i.e. the micro- and macro-tidal systems (Table 2). In "Estuary Suitability" section, we address the relevant estuarine characteristics for the suitability of a sill as salt intrusion mitigation measure.

Sill Placement

Whether a sill halts the salt intrusion or slows down its landward progression is in part determined by the dominant salt flux components, which are highly susceptible to the tidal range. For a smaller tidal range, the estuarine circulation dominates the landward salt flux (Fig. 5a). The estuarine circulation is driven by the density difference between salt and freshwater and is often referred to as the gravitational circulation (e.g. Hansen and Rattray 1965) as gravity is the driving force of this circulation. This aligns with the landward progression of the salt wedge being halted by the sill when the estuarine circulation is the driving force: The denser saline water flows underneath the lighter freshwater driven by gravity, but when the denser saline water meets an obstacle, it must overcome this gravitational pull to pass the barrier, i.e. the sill. As the driving force of the landward movement of the salt wedge—i.e. gravity—counteracts the upward movement of the salt wedge, the salt wedge movement (largely) vanishes when it meets the sill.

The landward—and subsequently seaward—momentum input from the tidal oscillations provides the salt wedge enough momentum to push the salt wedge over the sill. As this momentum is not gravity-driven, the driving force of the salt wedge does not disappear when meeting the sill. However, the sill functions as a sink of the tidal momentum causing the salt intrusion to be reduced with respect to an estuary without a sill (Fig. 3). When the estuarine circulation is the driving mechanism of the landward salt flux, the salt wedge experiences the sill as a 'wall', while the sill becomes a 'speed bump' for a tidally driven salt wedge.

When the sill is placed landward of the reference salt intrusion length, i.e. the salt intrusion length without a sill, it enhances the salt intrusion (Figs. 3 and 6). This behaviour originates from the sill blocking the seaward flow of freshwater in the lower part of the water column due to which the bottom saline water is experiencing less resistance to flow landward due to the sill implementation. Therefore, the sill's location in the estuary is crucial for its implementation, as a wrongly placed sill can enhance salt intrusion instead of mitigating it. Note that the enhancement of the salt intrusion

length is in the order of kilometres due to the local stimulation of the estuarine circulation (Figs. 3 and 6).

Sill Dimensions

Figure 4 presents the influence of the sill height on the salt intrusion, which shows that the sill becomes more effective for larger sill heights when $h_s/d_c \leq 0.5$; beyond this point, the sill does not improve ($a = 0.5$ m) or even enhances salt intrusion ($a = 4.0$ m). The increased salt intrusion for higher sills ($h_s/d_c > 0.5$) in case of a large tidal range ($a = 4.0$ m) results from the large difference in flow area over the sill between high and low water, where during low water, the sill substantially reduces the flow area and can even become emergent. This results in a push-over of (part of) the salt wedge, which can subsequently not fully return back over the sill trapping the saline water at the landward side of the sill. This is not as relevant in case of a small tidal range ($a = 0.5$ m), because (1) the difference in flow area over the sill between high and low water is smaller, and (2) there is less momentum to push the saline water over the sill. Hence, the higher sills ($h_s/d_c > 0.5$) perform similar to a sill blocking half the water depth ($h_s/d_c = 0.5$). Thus, increasing the sill height is beneficial until approximately halfway the water depth.

As a higher sill requires more sediment, is morphologically less stable, potentially impedes navigation, and increases construction costs, a lower but elongated sill might be preferred. Figure 8 shows the effect of the (relative) sill height in case the sill volume (V_s) is maintained by modifying the sill length; a sill length $W_s = 1000$ m in combination with a sill depth ratio $\delta_s = 0.5$ is used as reference (Table 1)—labelled V_s^0 in Fig. 8. Figure 8 shows that elongating the sill to compensate for a reduction in the sill height is not very effective, with negligible differences for larger sill heights ($h_s/d_c \geq 0.4$). Thus, the sill height remains the dominant factor in reducing the salt intrusion (Fig. 8)—in combination with the sill's location in the estuary (Fig. 3).

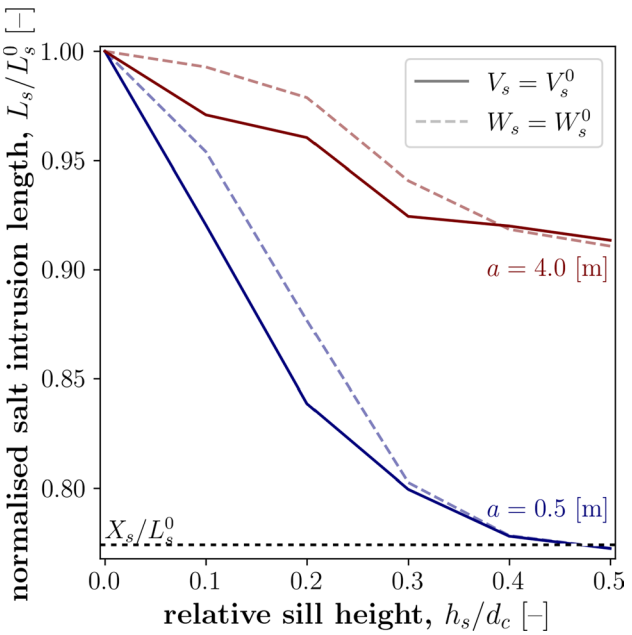

Fig. 8 Salt intrusion length for various sill heights while maintaining a constant sill volume for both tidal ranges. Dashed lines reflect the sills with a constant sill length (W_s^0) with $V_s \neq V_s^0$, as presented in Fig. 4

Estuary Suitability

Despite this study addressing idealised morphologies and a limited subset of estuary conditions, our results indicate that a sill shows the most promising implementation potential for salt wedge estuaries (Fig. 2). Here, the classification by Geyer and MacCready (2014) provides a better guide of suitability of a sill than the often used estuarine Richardson number. Sills are effective salt intrusion mitigation measures in both salt wedge and time-dependent salt wedge systems (Fig. 3), where the strength of the tidal component is inversely related to the efficacy of the sill. Therefore, we expect a sill as salt intrusion mitigation measure to be of interest in river-dominated estuaries, with decreasing efficacy for increasing tidal energy, e.g. in the Ebro River, the (Lower) Mississippi River, the Amazon River, and the Chang Jiang River (i.e. estuaries classified as [time-dependent]saltwedgein, Geyer and MacCready 2014, Fig. 6). Note, however, that the implementation of a sill might be constrained by other functions, such as the accessibility of a port and the required sill height (Fig. 4).

Conclusion

A (temporary) sill can be a viable solution in a salt wedge system, both micro- and macro-tidal (i.e. the investigated tidal ranges of 0.5 and 4.0 m, resp.). However, the efficacy of the sill to mitigate salt intrusion is reduced with increasing tidal range, i.e. tidal energy. This behaviour can be explained by analysing the salt flux components (Fig. 5): When salt transport is dominated by the estuarine circulation (F_3 in Eq. 3), the sill functions as a barrier—or wall—for the landward moving salinity, while salt transport dominated by the tidal oscillation (F_2 in Eq. 3) experiences the sill as a speed bump, reducing its landward momentum but not fully halting it. In other words, the stronger the salt wedge in the estuary, the more effective a sill is in mitigating salt intrusion.

A major constraint of the implementation of a sill is the required sill height: The sill must block a substantial part of the water column to be effective, with the sill height half of the water column resulting in the most effective mitigation (Fig. 4). This is related to the height of the salt wedge with

respect to the sill height. In addition, the longitudinal placement of the sill with respect to the expected salt intrusion length plays a major role in the efficacy of the sill: If the sill is placed seaward of the reference salt intrusion length ($X_s < L_s^0$), the salt intrusion reduces; otherwise ($X_s > L_s^0$), the sill *enhances* the salt intrusion (Figs. 3 and 6). As salt intrusion length predictions are still susceptible to large uncertainties, the location of the sill should be taken great care of.

Although a sill can be an effective mitigation measure to salt intrusion in various estuarine systems, the constraints on the placement and its height limit its widespread use. As many estuaries around the world provide just sufficient depth to accommodate vessel passage, the placement of a sill would result in unacceptable hindrance to these ports. Because the LMR is at places deeper than the maintained depth, the sill is a viable salt intrusion mitigation measure without obstructing vessel movements. Thus, despite the efficacy of a well-designed and well-placed sill to mitigate salt intrusion, socio-economic constraints limit its general viability as a mitigation measure during droughts.

Acknowledgements We are indebted to Peter M.J. Herman for his contributions to the research design, which greatly added value to the study and subsequent manuscript. In addition, we would like to thank Herman W.J. Kernkamp for his support with the hydrodynamic modelling software, Delft3D Flexible Mesh. The Tulane co-authors, Laura Manuel and Ehab Meselhe, are grateful for the opportunity to work with the TU Delft team on this research effort. The Tulane co-authors participated in this effort as part of the Mississippi River Delta Initiative -- MissDelta supported by the National Academy of Science. This work used the Dutch national e-infrastructure with the support of the SURF Cooperative using grant numbers EINF-4075 and EINF-7152. At last, we would also like to thank the two anonymous reviewers for their valuable feedback on the original manuscript; there suggestions greatly improved the manuscript.

Author Contributions G.H., S.P., S.A., E.M. designed the research; G.H. performed the research; G.H., L.M., S.P., S.A., E.M. analysed the data; G.H., wrote the manuscript; and G.H., L.M., S.P., S.A., E.M. reviewed the manuscript.

Funding This publication is part of the project 'Design and operation of nature-based SALTISolutions' (with project number P18-32 Project 7) of the research programme SALTISolutions which is (partly) financed by the Dutch Research Council (NWO).

Data Availability The dataset used in this study is publicly available Hendrickx et al. (2024): https://doi.org/10.4121/10d493df-8efb-442b-8c3d-04e92bcf4c4e.

Code Availability Processing code for the salt flux decomposition is open-source (Hendrickx 2023).

References

Costall, A., B. Harris, and J.P. Pigois. 2018. Electrical resistivity imaging and the saline water interface in high-quality coastal aquifers. *Surveys in Geophysics* 39 (4): 753–816. https://doi.org/10.1007/s10712-018-9468-0.

Deltares. 2022. Delft3D Flexible Mesh, User Manual.

Distefano, T., and S. Kelly. 2017. Are we in deep water? Water scarcity and its limits to economic growth. *Ecological Economics* 142: 130–147. https://doi.org/10.1016/j.ecolecon.2017.06.019.

Dronkers, J., and J. van de Kreeke. 1986. Experimental determination of salt intrusion mechanisms in the Volkerak estuary. *Netherlands Journal of Sea Research* 20 (1): 1–19. https://doi.org/10.1016/0077-7579(86)90056-6.

Fagerburg, T.L., and M.P. Alexander. 1994. *Underwater sill construction for mitigating salt wedge migration on the lower Mississipi River*. Hydraulic Laboratory, US Army Engineer Waterways Experiment Station, Vicksburg, MS, USA: Technical report.

Garcia, A.M.P. and W.R. Geyer. 2023. Tidal dispersion in short estuaries. *Journal of Geophysical Research: Oceans* 128:e2022JC018883. https://doi.org/10.1029/2022JC018883.

Garcia, A.M.P., W.R. Geyer, and N. Randall. 2021. Exchange flows in tributary creeks enhance dispersion by tidal trapping. *Estuaries and Coasts* 45 (2): 363–381. https://doi.org/10.1007/s12237-021-00969-4.

Geyer, W.R., and P. MacCready. 2014. The estuarine circulation. *Annual Review of Fluid Mechanics* 46 (1): 175–197. https://doi.org/10.1146/annurev-fluid-010313-141302.

Gong, W., and J. Shen. 2011. The response of salt intrusion to changes in river discharge and tidal mixing during the dry season in the Modaomen Estuary. *China. Continental Shelf Research* 31 (7–8): 769–788. https://doi.org/10.1016/j.csr.2011.01.011.

Haney, R.L. 1991. On the pressure gradient force over steep topography in sigma coordinate ocean models. *Journal of Physical Oceanography* 21 (4): 610–619. https://doi.org/10.1175/1520-0485(1991)021<0610:OTPGFO>2.0.CO;2.

Hansen, D.V., and M. Rattray Jr. 1965. Gravitational circulation in straits and estuaries. *Journal of Marine Research* 23: 104–122.

Hendrickx, G.G. 2023. NumPy-based salt flux decomposition.

Hendrickx, G.G., L.A. Manuel, S.G. Pearson, S.G.J. Aarninkhof, and E.A. Meselhe. 2024. Dataset underlying the study "An earthen sill as s measure to mitigate salt intrusion in estuatries" 4TU.ResearchData.Dataset. https://doi.org/10.4121/10d493df-8efb-442b-8c3d-04e92bcf4c4e.v1.

Hendrickx, G.G., W.M. Kranenburg, J.A.A. Antolínez, Y. Huismans, S.G.J. Aarninkhof, and P.M.J. Herman. 2023. Sensitivity of salt intrusion to estuary-scale changes: a systematic modelling study towards nature-based mitigation measures. *Estuarine, Coastal and Shelf Science* 295: 108564. https://doi.org/10.1016/j.ecss.2023.108564.

Johnson, B.H., M.B. Boyd, and G.H. Keulegan. 1987. *A mathematical study of the impact on salinity intrusion of deepening the lower Mississippi River navigation channel*. Hydraulic Laboratory, US Army Engineer Waterways Experiment Station, Vicksburg, MS, USA: Technical report.

Kernkamp, H.W.J., A. Van Dam, G.S. Stelling, and E.D. de Goede. 2011. Efficient scheme for the shallow water equations on

unstructured grids with application to the Continental Shelf. *Ocean Dynamics* 61 (8): 1175–1188. https://doi.org/10.1007/s10236-011-0423-6.

Lerczak, J.A., W.R. Geyer, and R.J. Chant. 2006. Mechanisms driving the time-dependent salt flux in a partially stratified estuary. *Journal of Physical Oceanography* 36 (12): 2296–2311. https://doi.org/10.1175/JPO2959.1.

Lerczak, J.A., W.R. Geyer, and D.K. Ralston. 2009. The temporal response of the length of a partially stratified estuary to changes in river flow and tidal amplitude. *Journal of Physical Oceanography* 39 (4): 915–933. https://doi.org/10.1175/2008JPO3933.1.

Maul, G.A. and I.W. Duedall. 2019. Demography of coastal populations, In *Encyclopedia of Coastal Science*, eds. Finkl, C.W. and C. Makowski, 692–700. Springer International Publishing. https://doi.org/10.1007/978-3-319-93806-6_115.

Ralston, D.K., W.R. Geyer, and J.A. Lerczak. 2010. Structure, variability, and salt flux in a strongly forced salt wedge estuary. *Journal of Geophysical Research: Oceans* 115 (6): C06005. https://doi.org/10.1029/2009JC005806.

Schulz, E., H.M. Schuttelaars, U. Gräwe, and H. Burchard. 2015. Impact of the depth-to-width ratio of periodically stratified tidal channels on the estuarine circulation. *Journal of Physical Oceanography* 45 (8): 2048–2069. https://doi.org/10.1175/JPO-D-14-0084.1.

Stelling, G.S., and J.A.T.M. van Kester. 1994. On the approximation of horizontal gradients in sigma co-ordinates for bathymetry with steep bottom slopes. *International Journal for Numerical Methods in Fluids* 18 (10): 915–935. https://doi.org/10.1002/fld.1650181003.

Valle-Levinson, A. 2008. Density-driven exchange flow in terms of the Kelvin and Ekman numbers. *Journal of Geophysical Research: Oceans 113*(C4). https://doi.org/10.1029/2007JC004144.

Veldkamp, T.I.E., Y. Wada, H. de Moel, M. Kummu, S. Eisner, J.C.J.H. Aerts, and P.J. Ward. 2015. Changing mechanism of global water scarcity events: Impacts of socioeconomic changes and inter-annual hydro-climatic variability. *Global Environmental Change* 32: 18–29. https://doi.org/10.1016/j.gloenvcha.2015.02.011.

Villemonte, J.R. 1947. Submerged-weir discharge studies. Engineering News. *Record* 139: 866–869.